

RESEARCH ARTICLE | NOVEMBER 20 2023

# Thermodynamic modeling of the Al–Cr–Mo–Ni system

Jian Peng ; Wei Huang ; Man Xu; Shulin Wang; Zhigang Xu; Wenjun Li; Junjun Wang  ; Chuanbin Wang; Peter Franke ; Hans J. Seifert



AIP Advances 13, 115022 (2023)

<https://doi.org/10.1063/5.0176225>



CrossMark

## AIP Advances

### Why Publish With Us?

-  **25 DAYS**  
average time to 1st decision
-  **740+ DOWNLOADS**  
average per article
-  **INCLUSIVE**  
scope

[Learn More](#)



# Thermodynamic modeling of the Al–Cr–Mo–Ni system

Cite as: AIP Advances 13, 115022 (2023); doi: 10.1063/5.0176225

Submitted: 12 September 2023 • Accepted: 26 October 2023 •

Published Online: 20 November 2023



View Online



Export Citation



CrossMark

Jian Peng,<sup>1,2</sup> Wei Huang,<sup>2</sup> Man Xu,<sup>1,3</sup> Shulin Wang,<sup>3</sup> Zhigang Xu,<sup>1</sup> Wenjun Li,<sup>4</sup> Junjun Wang,<sup>1,3,a)</sup> Chuanbin Wang,<sup>1,2</sup> Peter Franke,<sup>5</sup> and Hans J. Seifert<sup>5</sup>

## AFFILIATIONS

<sup>1</sup>Chaozhou Branch of Chemistry and Chemical Engineering Guangdong Laboratory, Chaozhou 521000, Guangdong, People's Republic of China

<sup>2</sup>State Key Lab of Advanced Technology for Materials Synthesis and Processing, Wuhan University of Technology, Wuhan 430070, People's Republic of China

<sup>3</sup>Hubei Key Laboratory of Plasma Chemistry and Advanced Materials, Engineering Research Center of Environmental Materials and Membrane Technology of Hubei Province, School of Materials Science and Engineering, Wuhan Institute of Technology, Wuhan 430074, People's Republic of China

<sup>4</sup>Qingdao Kairui Electronics Co., Ltd., Qingdao 266000, China

<sup>5</sup>Institute for Applied Materials - Applied Materials Physics, Karlsruhe Institute of Technology, Hermann-von-Helmholtz Platz 1, 76344 Eggenstein-Leopoldshafen, Germany

<sup>a)</sup>Author to whom correspondence should be addressed: [junjunwang@wit.edu.cn](mailto:junjunwang@wit.edu.cn)

## ABSTRACT

The Al–Cr–Mo–Ni system is of technical interest because it is an essential system for the thermodynamic modeling of systems related to the Ni- and NiAl-based superalloys. The knowledge of phase behaviors and thermodynamic properties of this system will be greatly helpful for the development of related alloys. Thermodynamic modeling of the Al–Cr–Mo–Ni system in the previous effort is not satisfactory. In this study, the Cr–Mo–Ni system was re-optimized with more sophisticated binary databases, and a new thermodynamic database of the Al–Cr–Mo–Ni system was established. A satisfactory agreement between calculated results and experimental data was obtained. The thermodynamic database developed in this study is suitable for assisting the design of both Ni- and NiAl-based superalloys.

© 2023 Author(s). All article content, except where otherwise noted, is licensed under a Creative Commons Attribution (CC BY) license (<http://creativecommons.org/licenses/by/4.0/>). <https://doi.org/10.1063/5.0176225>

## I. INTRODUCTION

Both Ni-based and NiAl-based superalloys have attracted intensive attention because of their exceptional physical and chemical properties at high temperatures.<sup>1–5</sup> The Al–Ni system serves as an essential basis for both alloys since the coexistence of cuboidal precipitates of the disordered *fcc* matrix (Ni-rich solid solution) and the ordered L1<sub>2</sub> (Ni<sub>3</sub>Al) phase and is the primary reason for the outstanding mechanical properties of Ni-based alloys and it covers the intermetallic compound NiAl. Cr and Mo are common alloying elements used to tailor the mechanical properties of Ni- and NiAl-based alloys.<sup>1</sup> As a result, creating a thermodynamic database that applies to both the Ni- and NiAl-based superalloys will provide

insights into their phase behaviors and thermodynamic properties and ease the research and design of both superalloys.

In the previous efforts by Havránková *et al.*,<sup>6</sup> the isothermal section (Ni = 70 at. %) at 1173 K was calculated. Although it seems that the predicted phase compositions are in good agreement with experiment data, several limitations exist. First, the used Al–Cr–Mo–Ni quaternary database is just a direct combination of thermodynamic datasets from Lu *et al.* (Al–Mo–Ni),<sup>7</sup> Frisk<sup>8</sup> (Cr–Mo–Ni), Dupin *et al.* (Al–Ni–Cr),<sup>9</sup> and Huang and Chang (Al–Ni)<sup>10</sup> without optimizing any new parameters, leading to the issue that the disordered (Ni) *fcc* phase of the Al–Cr–Mo–Ni system is falsely ordered. Second, although the combined database can well reproduce experimental observation in the Ni-rich region,

especially at 1173 K, but has an inferior representation of the remaining regions, especially the NiAl–Cr–Mo system.<sup>4,5,11–13</sup> Therefore, thermodynamic modeling of the Al–Cr–Mo–Ni system and re-optimization of necessary constituent ternary systems are demanded to establish a thermodynamic database that applies to both Ni- and NiAl-based superalloys.

In this work, CALPHAD modeling of the Al–Cr–Mo–Ni system is performed to provide a satisfactory thermodynamic description of both the Ni-rich and NiAl-rich corners. The constituent Cr–Mo–Ni system was re-optimized after critically evaluating available experimental data. The modeling of the ordered Ni<sub>3</sub>Al L1<sub>2</sub> phase is updated to ensure its disordered (Ni) fcc parent phase can be properly disordered in the whole Al–Cr–Mo–Ni system. The calculated results were compared with available experimental data.

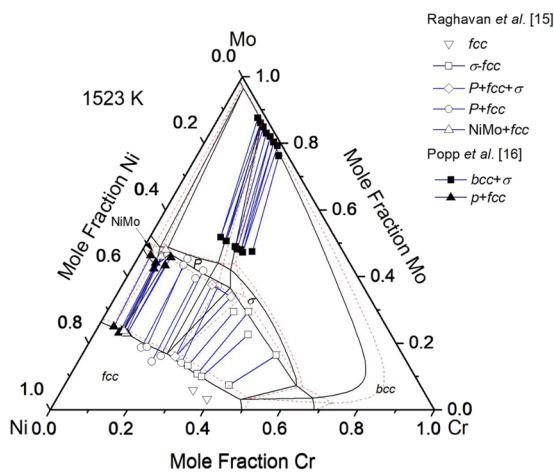


**FIG. 1.** Calculated isothermal section at 1523 K using the present thermodynamic description (solid lines) in comparison with that by Frisk<sup>3</sup> (dashed lines) and experimental data of Raghavan *et al.*<sup>15</sup> and Popp *et al.*<sup>16</sup>

## II. REVIEW OF THE Cr–Mo–Ni AND Al–Cr–Mo–Ni SYSTEMS

### A. Cr–Mo–Ni system

Bloom and Grant,<sup>14</sup> Raghavan *et al.*<sup>15</sup> and Popp *et al.*<sup>16</sup> constructed isothermal sections of this system at 1523 K based on experimental data. The isothermal section reported in Ref. 14 consists of six phases, i.e., bcc, fcc, a ternary extension of the binary NiMo phase, a ternary extension of the  $\beta$  phase from the Cr–Ni binary system, and two ternary phases ( $\sigma$  and  $P$ ). However, the existence of the  $\beta$  phase disaccords with the Cr–Ni phase diagram is accepted nowadays. The constructed isothermal sections at 1523 K in Refs. 14–16 are in reasonable agreement with each other. It is worth mentioning that a remarkably larger homogeneity range of the  $\sigma$  phase is reported in Ref. 16 than those by Bloom and Grant<sup>14</sup> and Raghavan

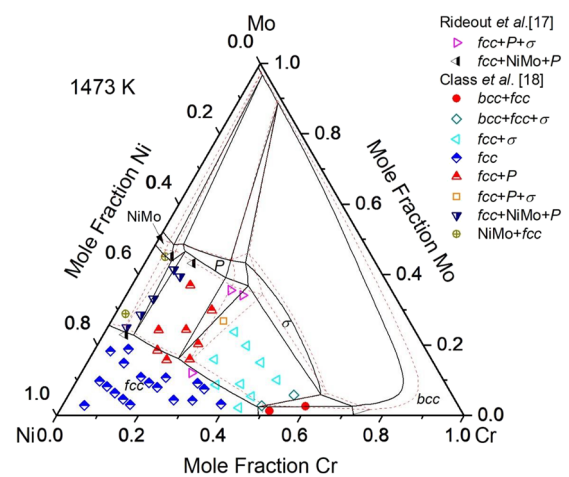


**FIG. 3.** Calculated isothermal section at 1473 K using the present thermodynamic description (solid lines)<sup>43</sup> in comparison with that by Frisk<sup>3</sup> (dashed lines) and the experimental data of Rideout *et al.*<sup>17</sup> and Class *et al.*<sup>18</sup>

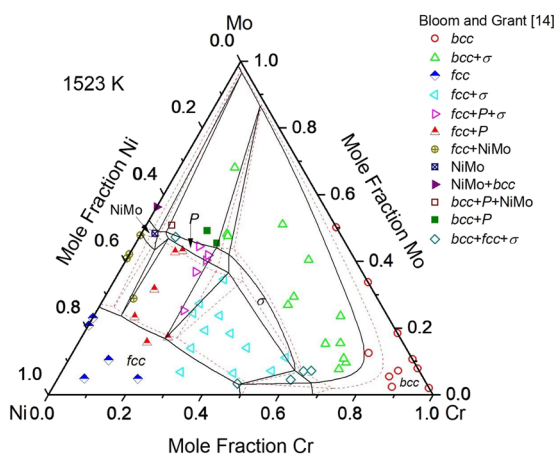


**FIG. 2.** Calculated isothermal section at 1523 K using the present thermodynamic description (solid lines)<sup>43</sup> in comparison with that by Frisk<sup>3</sup> (dashed lines) and the experimental data of Bloom and Grant.<sup>14</sup>

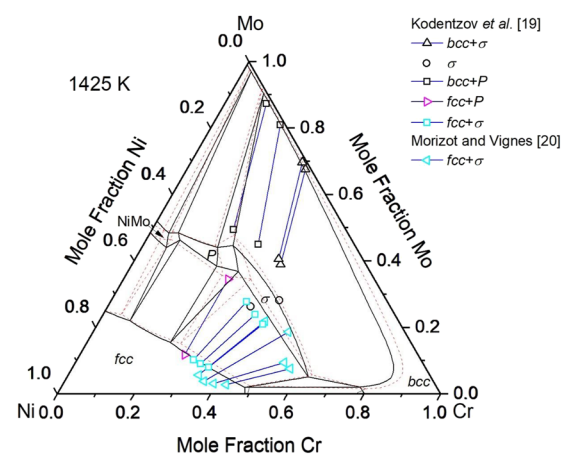


**FIG. 4.** Calculated isothermal section at 1425 K using the present thermodynamic description (solid lines)<sup>43</sup> in comparison with that by Frisk<sup>3</sup> (dashed lines) and the experimental data of Kodentzov<sup>19</sup> and Morizot and Vignes.<sup>20</sup>

*et al.*<sup>15</sup> A partial isothermal section at 1473 K of this system is constructed by Rideout *et al.*,<sup>17</sup> in which the homogeneity ranges of  $\sigma$  and  $P$  phases are in better agreement with those in Ref. 15 than those in Ref. 14. Also, it is observed that as temperature decreases, the homogeneity range of the  $\sigma$  phase shrinks.<sup>14,15,17</sup> Partial isothermal sections (>40 at. % Ni) at 1073, 1273, and 1473 K were experimentally determined by Class *et al.*,<sup>18</sup> and both  $\sigma$  and  $P$  were considered. The isothermal section at 1473 K in Refs. 17 and 18 agrees well with each other.

The  $\mu$  phase was detected at 1123 K<sup>15</sup> but was not observed at 1073 K,<sup>17</sup> meaning that this phase is stable above a temperature between 1073 and 1123 K. The isothermal section at 1425 K was constructed based on the experimentally determined tie-lines by diffusion couple technique,<sup>19</sup> which is in good agreement with tie-lines at 1423 K.<sup>20</sup> Tie-lines at 1373 K from Frisk<sup>8</sup> and Selleby<sup>21</sup> are consistent. The isothermal section at 873 K is determined by Goldschmidt.<sup>22</sup> A ternary phase designated A was also detected in addition to the  $\sigma$  and  $P$  phases. It claims the  $\sigma$  phase existed in a relatively vast field, which contradicted the previous findings.<sup>14,15,17</sup> Thus, both  $\mu$  and A phases are included in the present modeling.

Smiryagin *et al.*<sup>23</sup> constructed several partial vertical sections of the Cr–Mo–Ni system. However, only regions above 1473 K are in accord with those in Refs. 14, 15, and 17, and a significant discrepancy in the rest regions can be observed. Siedschlag<sup>24</sup> first created a partial liquidus projection of this system using measured melting temperatures of a serial of alloys containing less than 50 at. % Mo. However, the reference binary systems were insufficiently accurate and this projection differed significantly from later studies.<sup>14</sup> Bloom and Grant<sup>14</sup> updated the liquidus surface based on newly measured melting temperatures of ~100 Cr–Mo–Ni alloys and this liquidus surface is divided into five primary phase regions, i.e., NiMo,  $\sigma$ ,  $P$ ,  $bcc$ , and  $fcc$ . Alloy compositions with a melting temperature of 1673 K are available from Smiryagin *et al.*,<sup>23</sup> which accords well with data reported in Ref. 14. Based on experimental data<sup>14</sup> and liquidus data of constituent binary systems, both Chakravorty *et al.*<sup>25</sup> and Gupta<sup>26</sup> reconstructed the liquidus projection of this system.

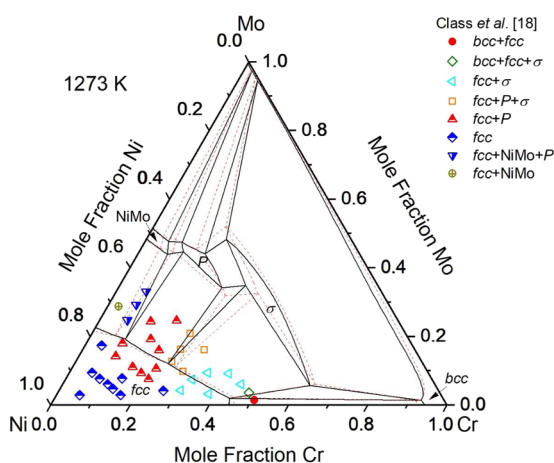


**FIG. 5.** Calculated isothermal section at 1273 K using the present thermodynamic description (solid lines)<sup>43</sup> in comparison with that by Frisk<sup>8</sup> (dashed lines) and the experimental data of Class *et al.*<sup>18</sup>

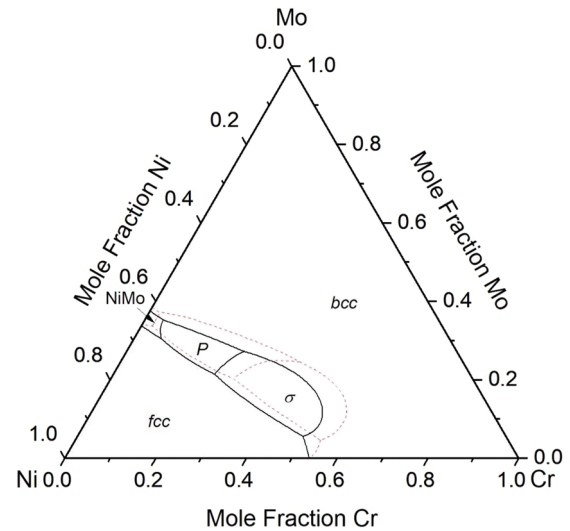


**FIG. 6.** Calculated liquidus projection using the present thermodynamic description (solid lines)<sup>43</sup> in comparison with that by Frisk<sup>8</sup> (dashed lines).

**TABLE I.** Calculated invariant reaction temperatures of the Cr–Mo–Ni system in this work.<sup>43</sup>

Reactions	Temperature (K)		
	Present work	Reference 25	Reference 26
Liquid + $bcc$ + $\sigma$ $\leftrightarrow$ $P$	1702	1733	1733
Liquid + $bcc$ + $P$ $\leftrightarrow$ NiMo	1620	1593	1593
Liquid $\leftrightarrow$ $fcc$ + $bcc$ + $\sigma$	1604	1615	1578
Liquid $\leftrightarrow$ $fcc$ + $P$ + $\sigma$	1602	1548	1548
Liquid + $P$ $\leftrightarrow$ $fcc$ + NiMo	1589	1573	1573

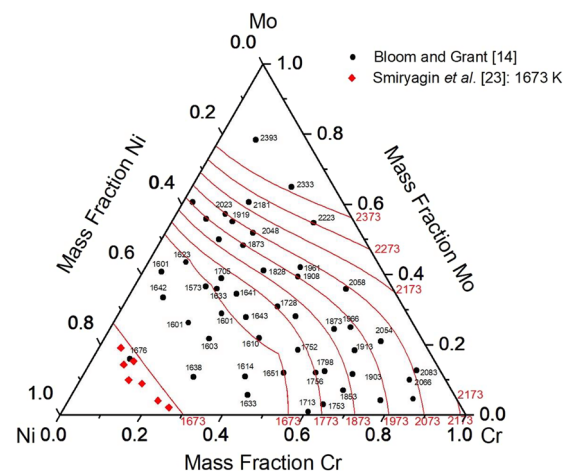


**FIG. 7.** Calculated isothermal lines (solid lines) of the Cr–Mo–Ni system using the present thermodynamic description<sup>43</sup> in comparison with the liquidus temperatures (units, K) measured by Bloom and Grant<sup>14</sup> and Smiryagin *et al.*<sup>23</sup>

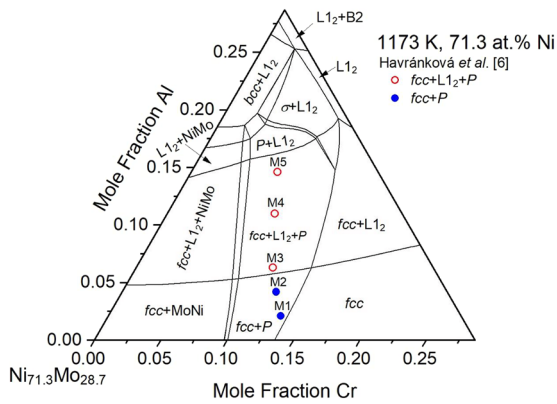


**FIG. 8.** Calculated 71.3 at. % Ni section of the system Al–Cr–Mo–Ni at 1173 K<sup>43</sup> in comparison with experimental data from Havránková *et al.*<sup>6</sup>

No thermodynamic data are experimentally determined for the Cr–Mo–Ni system. Kaufman and Nesor<sup>27</sup> modeled this system first using the CALPHAD approach. Later, Frisk<sup>8</sup> established a new database based on the thermodynamic data from SGTE (Scientific Group Thermodata Europe), and both ternary phases  $\sigma$  and  $P$  were considered. This database was further modified by Turchi *et al.*<sup>28</sup> However, because the binary Mo–Ni databases used in Refs. 8 and 28 differ from the respective choice in this study for the Al–Mo–Ni system,<sup>29</sup> the Cr–Mo–Ni system must be re-optimized to be compatible with other ternary systems of the Al–Cr–Mo–Ni quaternary system.

### B. Al–Cr–Mo–Ni system

The primary solidification surface of the NiAl–Cr–Mo system can be constructed with the primary solidified phases and

eutectic compositions of several NiAl–Cr–Mo alloys determined by Shang *et al.*,<sup>4</sup> Whittenberger *et al.*,<sup>5</sup> Wang *et al.*,<sup>11</sup> Zhang *et al.*,<sup>12</sup> and Peng *et al.*<sup>13</sup> Phases and their compositions of Al–Cr–Mo–Ni alloys with ~50,<sup>25,30</sup> 60,<sup>25,30</sup> and 75 at. % Ni<sup>31</sup> and equimolar Cr and Mo were studied by Chakravorty *et al.*<sup>25,30</sup> and Chakravorty and West<sup>31</sup> after annealing at 1073, 1273, and 1523 K, respectively. More than four phases appear in the majority of the annealed alloys with 50 and 60 at. % Ni, indicating that phase equilibria were not achieved because it defies the Gibbs phase rule that only equilibria with four or fewer phases are reasonable in a quaternary system. Thus, these data are excluded from the current modeling. Havránková *et al.*<sup>6</sup> reported the phase compositions of five Al–Cr–Mo–Ni alloys (~70 at. % Ni) after annealing at 1173 K for 300 h. Buršík and Svoboda<sup>32</sup> observed that the  $P$  and Ni<sub>2</sub>(Cr, Mo) phases existed in some Al–Cr–Mo–Ni alloys with 70 at. % Ni even after annealing at 873 or 1073 K up to 3000 h. No thermodynamic data on this quaternary system are reported.

### III. THERMODYNAMIC MODELING

Thermodynamic data of Al, Cr, Mo, and Ni were taken from the SGTE database.<sup>33</sup> The compound energy of vacancies ( $V_a$ ) was accepted by Franke.<sup>34</sup> A detailed explanation for this choice is given in Ref. 29 and, therefore, is omitted here. The Al–Cr–Mo–Ni system is comprised of four ternary systems, i.e., Al–Cr–Ni, Al–Cr–Mo, Al–Mo–Ni, and Cr–Mo–Ni. Available thermodynamic descriptions of these systems have been reviewed in Ref. 13. In this work, thermodynamic databases of Al–Cr–Ni,<sup>9</sup> Al–Mo–Ni,<sup>29</sup> and NiAl–Cr–Mo<sup>13</sup> systems were adopted and a re-optimization of the Cr–Mo–Ni system was performed. The ordered Ni<sub>3</sub>Al L1<sub>2</sub> phase and its disordered Al ( $fcc$ ) parent phase, both exhibiting  $fcc$  structure, were described with a single Gibbs energy function in the Al–Cr–Ni<sup>9</sup> and Al–Mo–Ni<sup>29</sup> systems and constraints between the parameters

**TABLE II.** Calculated phase compositions and their phase fraction (at. %) at 1173 K<sup>43</sup> in comparison with experimental data from Havránková *et al.*<sup>6</sup>  $f$ : Mole fraction of the corresponding phase.

Alloys	Phases	Calculated results					Experimental results				
		Al	Ni	Cr	Mo	$f$	Al	Ni	Cr	Mo	$f$
M1	$fcc$	2.2	71.6	12.8	13.4	95.5	1.7	71.0	12.4	15.0	99.0
	$P$	0	42.7	17.3	40.0	4.5	0.8	43.3	11.5	44.4	1.0
M2	$fcc$	4.3	72.3	11.4	12.0	96.8	3.6	72.4	11.4	12.5	99.0
	$P$	0	42.4	16.8	40.8	3.2	0.9	44.3	11.7	43.1	1.0
M3	$fcc$	6.1	72.8	10.3	10.8	89.4	5.4	70.6	11.7	12.3	87.4
	L1 <sub>2</sub>	18.0	74.8	3.7	3.5	4.9	16.7	73.9	2.9	6.6	11.4
	$P$	0	42.3	16.2	41.5	5.7	1.5	42.2	11.6	44.7	1.2
M4	$fcc$	6.1	72.6	10.7	10.6	46.9	5.6	70.1	13.5	10.8	47.3
	L1 <sub>2</sub>	18.0	74.8	3.8	3.4	45.3	17.7	73.3	3.3	5.8	49.0
	$P$	0	42.1	16.9	41.0	7.8	1.3	41.4	13.3	44.0	3.7
M5	$fcc$	6.2	72.2	11.6	10.0	17.7	7.1	68.7	15.7	8.5	17.6
	L1 <sub>2</sub>	18.0	74.6	4.2	3.2	75.0	17.2	74.0	3.9	5.0	78.4
	$P$	0	41.8	18.2	40.0	7.3	1.3	36.8	20.5	41.4	4.0

of the  $L_{12}$  phase were applied in these systems to guarantee that the disordered  $fcc$  phase is always correctly disordered. Similarly, such treatment is applied to the rest Cr–Mo, Al–Cr–Mo, Cr–Mo–Ni, and Al–Cr–Mo–Ni systems. The models used in this work are the same as those in the Cr–Mo–Ni,<sup>8</sup> Al–Cr–Ni,<sup>9</sup> Al–Mo–Ni,<sup>28</sup> and NiAl–Cr–Mo<sup>13</sup> system.

Substitutional solution phases, i.e., liquid,  $fcc$ , and  $bcc$  phases, were modeled with the formulations (Al, Cr, Mo, Ni), (Al, Cr, Mo, Ni), and (Al, Cr, Mo, Ni, Va), respectively. Their molar Gibbs energies are expressed as follows:

$$G_m = \sum_{i=1}^n x_i {}^0G_i + RT \sum_{i=1}^n x_i \ln x_i + {}^E G_m, \quad (1)$$

where  $x_i$  and  ${}^0G_i$  are the mole fractions of the pure elements (Al, Cr, Mo, and Ni) or Va and their corresponding molar Gibbs energies, respectively;  ${}^E G_m$  is the excess Gibbs energy and can be described by the following expression:

$${}^E G_m = {}^E G_m^{bin} + {}^E G_m^{tern} = \sum_{i=1}^{n-1} \sum_{j=i+1}^n x_i x_j L_{ij} + \sum_{i=1}^{n-2} \sum_{j=i+1}^{n-1} \sum_{k=j+1}^n x_i x_j x_k L_{ijk}, \quad (2)$$

where  ${}^E G_m^{bin}$  and  ${}^E G_m^{tern}$  represent the binary and ternary excess Gibbs energies, respectively.  $L_{ij}$  and  $L_{ijk}$  are binary and ternary interaction parameters, respectively. The binary interaction parameter  $L_{ij}$  with concentration dependence is expressed by the Redlich–Kister–Muggianu polynomial,<sup>35</sup>

$$L_{ij} = \sum_{v=0}^k (x_i - x_j)^v \cdot {}^v L_{ij}. \quad (3)$$

The  $\sigma$  and  $P$  in the Cr–Mo–Ni system were modeled as sublattice solution phases i.e.,  $(Ni)_8(Cr,Mo)_4(Cr,Mo,Ni)_{18}$  and  $(Cr,Ni)_{24}(Cr,Mo,Ni)_{20}(Mo)_{12}$ , respectively. The molar Gibbs energy can be expressed as

$$G_m = \sum_i y_i^I \sum_j y_j^II \sum_k y_k^III {}^0G_{i,j,k} + RT \sum_s \sum_i a^s y_i^s \ln y_i^s + {}^E G_m, \quad (4)$$

where the site fractions  $y_i^s$  and  $a^s$  are the composition of the respective sublattice (s) and the corresponding stoichiometric coefficients, respectively;  ${}^0G_{i,j,k}$  are the temperature-dependent compound energies of the respective end-members.<sup>36</sup> The  ${}^E G_m$  is expressed as

$${}^E G_m = \sum_i y_i^I \sum_j y_j^II \sum_k y_k^III \left[ \sum_{l>i} y_l^I \sum_v {}^v L_{i,l,j;k} (y_i^I - y_l^I)^v + \sum_{l>j} y_l^II \sum_v {}^v L_{i,j,l;k} (y_j^II - y_l^II)^v + \sum_{l>k} y_l^III \sum_v {}^v L_{i,j;k,l} (y_k^III - y_l^III)^v \right], \quad (5)$$

where ternary interaction parameters like  ${}^v L_{i,l;*,*}$  denote the  $v$ th interaction between the constituents  $i$  and  $l$  in the respective sublattice.

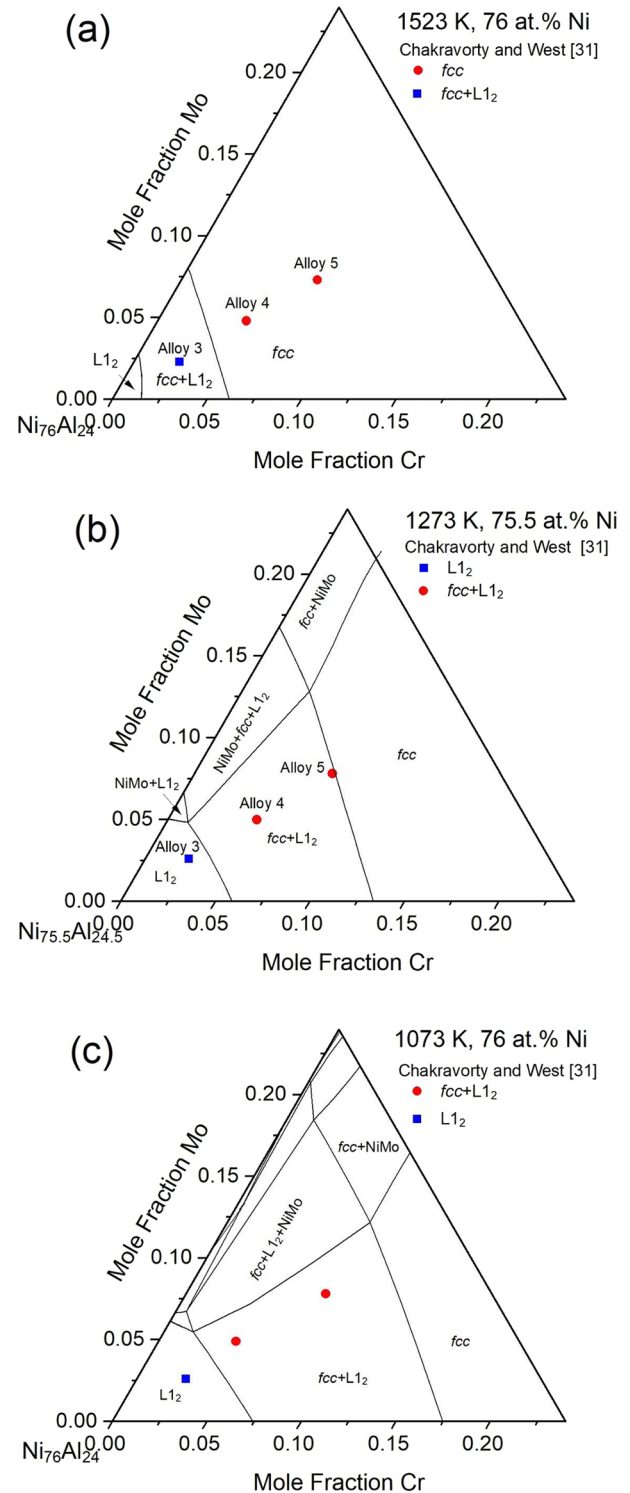


FIG. 9. Calculated isopleths of the Al–Cr–Mo–Ni system with (a) 76 at. % Ni section at 1523 K, (b) 75.5 at. % Ni section at 1273 K, and (c) 76 at. % Ni section at 1073 K in comparison with the experimental data.<sup>43</sup>

#### IV. OPTIMIZATION RESULTS AND DISCUSSION

Thermodynamic parameters were evaluated by the optimization module PARROT<sup>37</sup> and the diagrams were calculated by the software package Thermo-Calc.<sup>38,39</sup>

##### A. Cr–Mo–Ni system

As discussed in Sec. II A, only the ternary  $\sigma$  and  $P$  phases are considered with the  $\mu$  phase being ignored due to the discrepancy at low temperatures. The initial dataset for the optimization was a combination of the binary Cr–Ni,<sup>40</sup> Mo–Ni,<sup>41</sup> and Cr–Mo<sup>42</sup> datasets and the original parameters of the ternary  $\sigma$  and  $P$  phases from Frisk.<sup>8</sup> It was found that the  $P$ -NiMo equilibria determined by the initial dataset were erroneous as the dataset indicates that there is no solubility of Cr in the NiMo phase. Moreover, the homogeneity ranges of  $\sigma$ ,  $P$ , and  $fcc$  phases are not satisfactory. Thus, ternary interaction parameters of the  $P$  phases were optimized to ensure that NiMo can extend into the ternary system with a proper homogeneity range.<sup>14,15,18</sup> Next, the ternary interaction parameters of the  $\sigma$  and  $fcc$  phases were adjusted to fit the  $fcc$ - $\sigma$  equilibrium.<sup>14,15,18</sup> It is worth mentioning that, during parameters optimization, we observed if the  $\sigma$  phase is stabilized at low Cr region so that to reproduce its large homogeneity range reported by Popp *et al.*,<sup>16</sup> the calculated results of the Al–Cr–Mo–Ni quaternary system will deviate considerably from experimental results. Thus, in this work, the ternary interaction parameters optimization of the  $P$ ,  $\sigma$ , and  $fcc$  are mainly based on the data from Refs. 14, 15, and 18. Next, ternary interaction parameters of the liquid phase were optimized to fit the liquidus temperatures determined in Refs. 14 and 23. To make sure the  $fcc$  disordered state is always possible, the  $L1_2$  phase was modeled as a metastable phase in the Cr–Mo–Ni system. Since the calculated results agree well with experimental data, all ternary parameters were set to zero for the sake of simplicity. Finally, all parameters were

re-optimized simultaneously to reproduce all accepted experimental data.

Figures 1–5 show the calculated isothermal sections of the Cr–Mo–Ni system at 1523, 1473, 1425, and 1273 K using the present thermodynamic description (solid lines) in comparison with those of Frisk (dashed lines) and experimental data.<sup>43</sup> Calculated Cr solubility in the NiMo phase in this work is in better agreement with experimental results<sup>15</sup> than that in Ref. 8, as well as the homogeneity ranges of the  $bcc$  and  $fcc$  phases. Figure 4 indicates that the homogeneity range of the  $\sigma$  phase at 1425 K should be wider than expected in this work. In Fig. 5, the phase boundary of the  $fcc$  phase is not in good agreement with the experimental data. Since the constituent binary systems in this work are well determined, it seems the accuracy of the experimentally determined phase boundary is questionable.

Figure 6 shows the calculated liquidus projection using the current thermodynamic database (solid lines)<sup>43</sup> and that by Frisk<sup>8</sup> (dashed lines) is superimposed for comparison. A larger primary solidification region of the NiMo phase is achieved than that of Frisk,<sup>8</sup> while that of the  $P$  phase shrinks. Table I gives the invariant reaction temperatures of the Cr–Mo–Ni system determined in this study, which we believe are satisfactory because invariant reaction temperatures reported in Refs. 25 and 26 are estimates based on alloys melting points determined in Ref. 14 and liquidus data of constituent binary systems, which may be inaccurate. Figure 7 shows the calculated isothermal lines of the liquid phase in the Cr–Mo–Ni system without introducing ternary interaction parameters.<sup>43</sup> The melting temperatures from Bloom and Grant<sup>14</sup> and Smiryagin *et al.*<sup>23</sup> were also superimposed for comparison. A satisfactory agreement between the calculation and the experimental data was obtained, indicating that it is not necessary to include any ternary interaction parameters for the liquid phase in the present optimization. Such treatment is also adopted by Frisk.<sup>8</sup>

TABLE III. Calculated phase compositions<sup>43</sup> in comparison with experimental data from Chakravorty and West.<sup>31</sup>

Alloys	Temperature (K)	Phases	Calculated results				Experimental results			
			Al	Ni	Cr	Mo	Al	Ni	Cr	Mo
Alloy 3	1523	$fcc$	17.1	76.7	3.3	2.9	16.6	76.6	3.6	3.2
		$L1_2$	21.5	74.7	1.9	1.9	20.8	74.8	2.2	2.2
	1273	$L1_2$	19.9	75.2	2.3	2.6	19.9	75.2	2.3	2.6
		$L1_2$	18.9	75.9	2.6	2.6	18.9	75.9	2.6	2.6
Alloy 4	1523	$fcc$	14.2	76.3	4.7	4.8	14.2	76.3	4.7	4.8
		$fcc$	9.6	76.4	6.9	7.1	11.4	76.1	6.5	6.0
	1273	$L1_2$	18.5	75.3	2.9	3.3	17.2	74.7	3.6	4.5
		$fcc$	5.1	78.1	7.9	8.9	10.6	77.3	6.3	5.8
Alloy 5	1523	$L1_2$	16.9	75.8	3.3	4.0	16.3	76.0	3.5	4.2
		$fcc$	9.5	76.0	7.2	7.3	9.5	76.0	7.2	7.3
	1273	$fcc$	9.2	75.5	7.4	7.9	8.2	76.2	7.6	8.0
		$L1_2$	18.6	75.1	3.0	3.3	17.9	74.2	3.5	4.4
1073	$fcc$	4.6	76.1	9.4	9.9	6.8	76.4	8.5	8.3	
	$L1_2$	16.9	75.5	3.7	3.9	12.9	75.3	5.6	6.2	

## B. Al-Cr-Mo-Ni system

Figure 8 shows the comparison of the calculated 71.3 at. % Ni isopleth of the Al-Cr-Mo-Ni system at 1173 K with experimental data.<sup>43</sup> The calculation and experimental results (as listed in Table II<sup>43</sup>) are in excellent agreement. Not only does the composition of each phase coincide with the experimental results but so do their molar fractions. Because Al is taken into account in the modeling of the *P* phase, the calculated content of Al in the *P* phase in all alloys is zero. However, experimental observation indicates the Al solubility in the *P* phase is extremely small; therefore, our calculated results are acceptable.

Figure 9 shows the comparison of the calculated isopleths at ~76 at. % Ni of the Al-Cr-Mo-Ni system at 1523, 1273, and 1073 K with the experimental data.<sup>43</sup> The calculated phase compositions and experimental data are presented in Table III. Overall, the present thermodynamic description of the Al-Cr-Mo-Ni system can accurately predict the phase compositions. The *fcc* + *L1*<sub>2</sub> two-phase region, i.e., the  $\gamma$ - $\gamma'$  region, in this system, which is critical for the development of Ni-based superalloys, is thoroughly characterized. The computed partial isopleths differ significantly from those in Ref. 31 because more sophisticated thermodynamic descriptions of the constituent systems were used in this study.

Figure 10 shows the comparison of the calculated liquidus projection of the 62 at. % Ni section of the Al-Cr-Mo-Ni system using the current thermodynamic description and experimental data.<sup>43</sup> Our calculated results agree quite well with experimental results. The solidification process of the alloys was qualitatively modeled using the Scheil module in Thermo-Calc software. The results show that alloys #1 and #2 have ~76 and 50 at. % B2 phase, respectively, which is in reasonable agreement with the report of Chakravorty *et al.*<sup>25</sup> that alloy #1 has more B2 phase than alloy #2.

Furthermore, the current database can accurately reproduce the experimental data from the NiAl-Cr-Mo system. Figure 11 shows the comparison of the predicted partial liquidus projection of the NiAl-Cr-Mo system and published experimental data.<sup>43</sup> The calculated eutectic trough (solid black line) moves through the eutectic

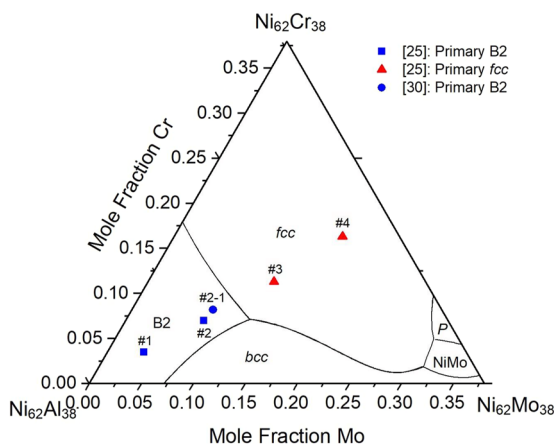


FIG. 10. Calculated liquidus surface projection of the 62 at. % Ni section of the Al-Cr-Mo-Ni system using the present description<sup>43</sup> in comparison with experimental data.<sup>25,30</sup>

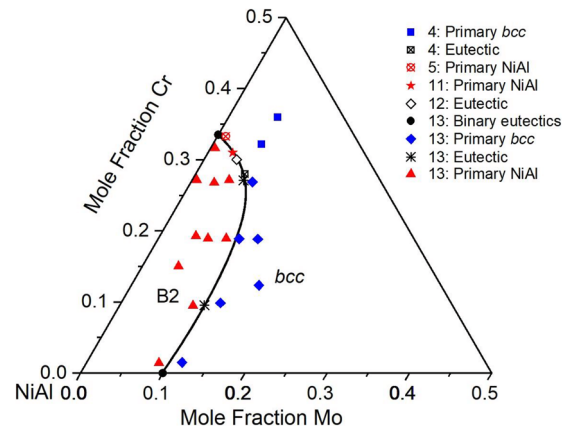


FIG. 11. Calculated partial liquidus projection of the NiAl-Cr-Mo system<sup>43</sup> in comparison with literature data.

compositions and separates alloys with primary solidified B2 and bcc phases, indicating that an excellent agreement between the calculation and experimental data is attained.

## V. CONCLUSION

Thermodynamic modeling of the Al-Cr-Mo-Ni and re-optimization of the Cr-Mo-Ni system were performed based on the CALPHAD approach. A more sophisticated thermodynamic description of the binary Mo-Ni is adopted and ternary parameters of the Cr-Mo-Ni system were re-optimized accordingly. The calculated phase diagrams of the Cr-Mo-Ni system are in better agreement with experimental data than the previous modeling. The constraints on the parameters of the ordered Ni<sub>3</sub>Al *L1*<sub>2</sub> phase were applied to the Al-Cr-Mo-Ni system and its sub-systems. Consequently, the disordered (Ni) *fcc* phase can be properly disordered in the whole system. Both calculated isothermal sections of the Ni-rich corner and the liquidus projections of the NiAl-Cr-Mo system can well reproduce available experimental data. Thus, a thermodynamic database of the Al-Cr-Mo-Ni system that applies to the design of both Ni- and NiAl-based superalloys was established.

## ACKNOWLEDGMENTS

This work was financially supported by the Guangdong Major Project of Basic and Applied Basic Research (Grant No. 2021B0301030001), the Self-innovation Research Funding Project of Hanjiang Laboratory (Grant No. HJL202202A003), and the Initiative and Networking Fund of the Helmholtz Association (Grant No. VH-KO-610).

## AUTHOR DECLARATIONS

### Conflict of Interest

The authors have no conflicts to disclose.



## Author Contributions

**Jian Peng:** Formal analysis (equal); Investigation (equal); Software (equal); Validation (equal); Writing – original draft (equal). **Wei Huang:** Formal analysis (equal); Validation (equal); Writing – review & editing (equal). **Man Xu:** Writing – review & editing (equal). **Shulin Wang:** Writing – review & editing (equal). **Zhigang Xu:** Validation (equal); Writing – review & editing (equal). **Wenjun Li:** Writing – review & editing (equal). **Junjun Wang:** Formal analysis (equal); Writing – original draft (equal); Writing – review & editing (equal). **Chuanbin Wang:** Funding acquisition (equal); Supervision (equal); Writing – review & editing (equal). **Peter Franke:** Conceptualization (equal); Supervision (equal); Writing – review & editing (equal). **Hans J. Seifert:** Conceptualization (equal); Funding acquisition (equal); Supervision (equal); Writing – review & editing (equal).

## DATA AVAILABILITY

The data that support the findings of this study are available from the corresponding author upon reasonable request.

## REFERENCES

- T. M. Pollock and S. Tin, “Nickel-based superalloys for advanced turbine engines: Chemistry, microstructure and properties,” *J. Propul. Power* **22**, 361–374 (2006).
- J.-M. Yang, “The mechanical behavior of in-situ NiAl-refractory metal composites,” *JOM* **49**, 40–43 (1997).
- X. F. Chen, D. R. Johnson, R. D. Noebe, and B. F. Oliver, “Deformation and fracture of a directionally solidified NiAl–28Cr–6Mo eutectic alloy,” *J. Mater. Res.* **10**, 1159–1170 (1995).
- Z. Shang, J. Shen, L. Wang, Y. Du, Y. Xiong, and H. Fu, “Investigations on the microstructure and room temperature fracture toughness of directionally solidified NiAl–Cr(Mo) eutectic alloy,” *Intermetallics* **57**, 25–33 (2015).
- J. D. Whittenberger, S. V. Raj, I. E. Locci, and J. A. Salem, “Elevated temperature strength and room-temperature toughness of directionally solidified Ni–33Al–33Cr–1Mo,” *Metall. Mater. Trans. A* **33**, 1385–1397 (2002).
- J. Havráňková, J. Buršík, A. Kroupa, and P. Brož, “Experimental study and thermodynamic assessment of the Ni–Al–Cr–Mo system at 1173 K,” *Scr. Mater.* **45**, 121–126 (2001).
- X. Lu, Y. Cui, and Z. Jin, “Experimental and thermodynamic investigation of the Ni–Al–Mo system,” *Metall. Mater. Trans. A* **30**, 1785–1795 (1999).
- K. Frisk, Report No. TRITA-MAC 429 (Royal Institute of Technology, Stockholm, Sweden, 1990).
- N. Dupin, I. Ansara, and B. Sundman, “Thermodynamic re-assessment of the ternary system Al–Cr–Ni,” *Calphad* **25**, 279–298 (2001).
- W. Huang and Y. A. Chang, “A thermodynamic analysis of the Ni–Al system,” *Intermetallics* **6**, 487–498 (1998).
- J. Wang, G. Zhang, and S. Li, “Investigation of microstructure and corrosive behavior of NiAl–31Cr–3Mo alloy at high temperature,” *Min. Metall. Eng.* **30**, 93–96 (2010).
- Z. Zhang, X. Liu, S. Gong, and H. Xu, “Microstructure and properties of the  $\beta$  NiAl and its eutectic alloy with Cr and Mo additions,” *Trans. Nonferrous Met. Soc. China* **16**, s2046–s2049 (2006).
- J. Peng, P. Franke, and H. J. Seifert, “Experimental investigation and CALPHAD assessment of the eutectic trough in the system NiAl–Cr–Mo,” *J. Phase Equilib. Diffus.* **37**, 592–600 (2016).
- D. S. Bloom and N. J. Grant, “An investigation of the systems formed by chromium, molybdenum, and nickel,” *J. Metals* **6**, 261–268 (1954).
- M. Raghavan, R. Mueller, G. A. Vaughn, and S. Floreen, “Determination of isothermal sections of nickel rich portion of Ni–Cr–Mo system by analytical electron microscopy,” *Metall. Trans. A* **15**, 783–792 (1984).
- R. Popp, S. Haas, F. Scherm, A. Redermeier, E. Povoden-Karadeniz, T. Gohler, and U. Glatzel, “Determination of solubility limits of refractory elements in TCP phases of the Ni–Mo–Cr ternary system using diffusion multiples,” *J. Alloys Compd.* **788**, 67–74 (2019).
- S. Rideout, W. D. Manly, E. L. Kamen, B. S. Lement, and P. A. Beck, “Intermediate phases in ternary alloy systems of transition elements,” *JOM* **3**, 872–876 (1951).
- I. Class, H. Gräfen, and E. Scheil, “Entwicklung einer ausscheidungsträgen korrosionsbeständigen Nickel–Chrom–Molybdän–Legierung,” *Int. J. Mater. Res.* **53**, 283–293 (1962).
- A. A. Kodentsov, S. F. Dunaev, and E. M. Slusarenko, “Diffusion paths and phase equilibria in the Mo–Ni–Cr system at 1425 K,” *J. Less-Common Met.* **141**, 225–234 (1988).
- C. Morizot and A. Vignes, “Study of the Ni–Co–Cr–Mo diagram from the point of view of predicting the appearance of sigma phase in super-refractory alloys,” *Mem. Sci. Rev. Met.* **70**, 857–874 (1973).
- M. Selleby, Bachelor Thesis, Division of Physical Metallurgy (Royal Institute of Technology, Stockholm, Sweden, 1982).
- H. J. Goldschmidt, in *Metallurgy of Rare Metals I: Chromium*, edited by A. H. Shully (Butterworths Publishing Company, London, 1954).
- A. P. Smiryagin, A. Ya. Potinkin, and R. P. Martinuk, “The Ni–Mo–Cr phase diagram,” *Zhur, Neorg. Khim* **3**, 853–859 (1958).
- E. Siedschlag, “Das dreistoffsystem chrom–nickel–molybdän,” *Z. Metallkde.* **17**, 53–56 (1925).
- S. Chakravorty, S. Sadiq, and D. R. F. West, “Equilibria involving P- and  $\sigma$ -phases in Ni–Cr–Al–Mo system,” *Mater. Sci. Technol.* **2**, 110–121 (1986).
- K. P. Gupta, *Phase Diagrams of Ternary Nickel Alloys, Part I* (Indian Institute of Metals, 1990), pp. 26–48.
- L. Kaufman and H. Nesor, “Calculation of superalloy phase diagrams: Part I,” *Metall. Trans.* **5**, 1617–1721 (1974).
- P. Turchi, L. Kaufman, and Z.-K. Liu, “Modeling of Ni–Cr–Mo based alloys: Part I—Phase stability,” *Calphad* **30**, 70–87 (2006).
- J. Peng, P. Franke, D. Manara, T. Watkins, R. J. M. Konings, and H. J. Seifert, “Experimental investigation and thermodynamic re-assessment of the Al–Mo–Ni system,” *J. Alloys Compd.* **674**, 305–314 (2016).
- S. Chakravorty, S. Sadiq, and D. R. F. West, “Intermetallic compound precipitation in Ni–Cr–Al–Mo system,” *Mater. Sci. Technol.* **3**, 629–641 (1987).
- S. Chakravorty and D. R. F. West, “The Ni<sub>3</sub>Al–Ni<sub>3</sub>Cr–Ni<sub>3</sub>Mo section of the Ni–Cr–Al–Mo system,” *J. Mater. Sci.* **19**, 3574–3587 (1984).
- J. Buršík and M. Svoboda, “The existence of P phase and Ni<sub>2</sub>Cr superstructure in Ni–Al–Cr–Mo system,” *Scr. Mater.* **39**, 1107–1112 (1998).
- A. Dinsdale, “SGTE data for pure elements,” *Calphad* **15**, 317–425 (1991).
- P. Franke, “Modeling of thermal vacancies in metals within the framework of the compound energy formalism,” *J. Phase Equilib. Diffus.* **35**, 780–787 (2014).
- O. Redlich and A. T. Kister, “Algebraic representation of thermodynamic properties and the classification of solutions,” *Ind. Eng. Chem.* **40**, 345–348 (1948).
- M. Hillert, “The compound energy formalism,” *J. Alloys Compd.* **320**, 161–176 (2001).
- B. Jansson, Ph.D. thesis, Royal Institute of Technology, Stockholm, 1983.
- J.-O. Andersson, T. Helander, L. Höglund, P. Shi, and B. Sundman, “Thermo-Calc & DICTRA, computational tools for materials science,” *Calphad* **26**, 273–312 (2002).
- B. Sundman, B. Jansson, and J.-O. Andersson, “The Thermo-Calc databank system,” *Calphad* **9**, 153–190 (1985).
- B. Lee, “On the stability of Cr carbides,” *Calphad* **16**, 121–149 (1992).
- S. H. Zhou, Y. Wang, C. Jiang, J. Z. Zhu, L. Q. Chen, and Z. K. Liu, “First-principles calculations and thermodynamic modeling of the Ni–Mo system,” *Mater. Sci. Eng.: A* **397**, 288–296 (2005).
- K. Frisk and P. Gustafson, “An assessment of the Cr–Mo–W system,” *Calphad* **12**, 247–254 (1988).
- B. Jansson, Ph.D. thesis, Karlsruhe Institute of Technology, Karlsruhe, 2016.